

The Relevance of Measurement Systems Analysis

A Procter & Gamble Case Study on
MSA Methodology and Applications

DATE

**OCTOBER
10 AND 12**

TIME

**16:00 CET,
10 am EST**



**CHRISTIAN
NEU**

Scientist
Procter & Gamble



**JERRY
FISH**

Systems Engineer
JMP



**JASON
WIGGINS**


Senior Systems
Engineer
JMP

[Register now](#)

Damian Pieloth^{1,2}
Matthias Rodeck¹
Gerhard Schaldach¹
Markus Thommes^{1,*}

Categorization of Sprays by Image Analysis with Convolutional Neuronal Networks

Spray characterization has been an issue for process and product characterization for decades. Because of this, a convolutional neuronal network was developed to determine the droplet size from spray images. The images were taken using a digital camera, a light source, and a dark room. These were subsequently employed to design and train a convolutional neuronal network using open-source software packages and a desktop computer. The accuracy of the network droplet size determinations was checked with additional, independent images. The median drop size was assessed with a high accuracy of more than 99.8 % as the mean spray performance indicator. Additionally, the droplet size distribution measurements from the neural network method deviated from those from the reference method (laser diffraction) by less than 1.5 %. Convolutional neuronal networks can be applied to determine the spray performance using spray cone images. This approach could be useful for multiple applications.

 This is an open access article under the terms of the Creative Commons Attribution-NonCommercial-NoDerivs License, which permits use and distribution in any medium, provided the original work is properly cited, the use is non-commercial and no modifications or adaptations are made.

Keywords: Convolutional neural networks, Droplet size, Image analysis, Machine learning, Spray categorization

Received: July 28, 2022; *revised:* September 19, 2022; *accepted:* November 02, 2022

DOI: 10.1002/ceat.202200356

1 Introduction

The atomization of liquids is one of the basic operations in process engineering. The spray produced by a given atomizer depends essentially on its geometry, the operating conditions, and the material properties of the atomized liquids. The spray properties, such as drop size or spraying angle, must fulfil specific requirements for each unique application [1].

Medical spray pumps for pharmaceutical applications are widely used to administer drugs into the lungs, the throat or the nose. These nebulizers are employed to deliver drug solutions to the mucosa, and their performance depends on the droplet size and velocity [2]. In pulmonary (lung) applications the goal is droplet sizes of about 3 μm with a low droplet velocity, since larger particles are deposited in the upper airways while smaller particles are preferentially inhaled into the alveoli [3, 4]. Single-phase swirl nozzles (hollow-cone or full-cone nozzles) are commonly used in medical nebulizers, and guidelines from the regulatory authorities are in place, which specify the aerodynamic droplet diameter as a critical quality attribute [5].

Therefore, the droplet size and the spray-cone geometry are frequently measured for each unit as part of process control during the production of pharmaceutical nebulizers. However, conventional methods like laser diffraction and phase Doppler anemometer analysis are insufficient to keep up with the high production rates of spray pumps at this time. Due to this fact, new technologies for spray characterization that are both reliable and fast are needed.

One rather new and promising approach for droplet characterization is image analysis, which has been successfully applied in fields such as diesel sprays, emulsions, simulated rain, and

thermal coatings [6, 7]. It has been proven that common issues such as sample preparation, errors caused by dense sprays, non-spherical drops, or high drop velocities can be avoided [8]. Algorithms allowing precise automatic particle size measurement in real time have been developed, and the automatic counting and measuring of particles in multiphase systems has been introduced [9].

The issue with classical image analysis is the complexity of the evaluation algorithms, as well as the time needed to analyze the data. These problems can be overcome using machine learning (ML) algorithms which are, additionally, highly adaptable for various other applications and tasks [10]. In the literature, complex multiphase flows have been characterized with image analysis via machine learning algorithms. Unnikishnan et al. [11] provide a system characterizing an emulsification process by determining drop sizes done by an ML algorithm.

Neural networks (NNs) are a subcategory of machine learning. These consist of a stack of layers, each one having various numbers of neurons connected with the other neurons in the previous and subsequent layer, forming a so-called full connected layer [12]. The connections are weighted, giving the opportunity to train the neuronal net iteratively.

¹Prof. Dr.-Ing. Damian Pieloth, Matthias Rodeck, Gerhard Schaldach, Prof. Dr. Markus Thommes
(professors.fsv.bci@tu-dortmund.de)
Technical University Dortmund, Laboratory of Solids Process Engineering, Emil-Figge-Str. 68, 44227 Dortmund, Germany.

²Prof. Dr.-Ing. Damian Pieloth
Hochschule Anhalt, Bernburger Str. 55, 06366 Köthen, Germany.

Image analysis with convolutional neuronal networks (CNNs) has been successfully applied in fields such as facial recognition, autonomous driving, and cancer detection [13–15]. Based on this, CNNs should be suitable for spray characterization by images. However, regular images are rather large with respect to data size and include information unnecessary for spray characterization. A data pretreatment is required to reduce the data size while highlighting relevant information (features) of the images. Therefore, additional layers are implemented in CNNs designed for image handling (Fig. 1).

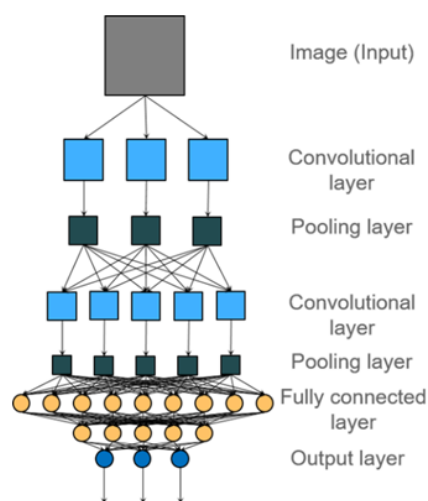


Figure 1. Schematic structure of a neural network for image recognition consisting of convolutional and pooling layers followed by the fully connected neurons with adjustable weights and the output layer.

During convolution, the image is treated as a two-dimensional matrix (input feature map) and convoluted with a second matrix (kernel), resulting in a third matrix (output feature map). During this linear transformation, notation and ordering of the contributions (relevant features) are preserved. The subsequent pooling step reduces the data size of the output feature map by summarizing sub-regions, such as the maximum value (max. pooling), as used in this application. The purpose of the fully connected layer is to interpret the features by categorizing them into predefined labels, such as droplet size or spray angle. The results are mapped to a target function by the output layer, which is an integral part of each neuronal network.

NNs must be trained to specific applications using an iterative algorithm. Therefore, multiple images with known labels (droplet size) are subsequently presented to the CNN. During the training, the connections between the individual neurons are weighted, and the success of the weighting process is verified by a subsequent validation. These two steps are called an epoch, while CNNs are trained over several epochs in an iteration process. Finally, the CNN can apply the learned rules to unlabeled images and categorize those with respect to labels, based on the features of the images used in the training. Due to the high CPU requirement, graphic cards are often used to accelerate the training of the CNNs [16].

The aim of this work is to develop and implement an optical quality control system, capable of characterizing sprays with a

predefined specification. Therefore, a measuring framework for spray images should be developed and a CNN should be established to determine the median drop diameter of the volume distribution. These parameters were used as an indicator of the performance of a specific unit during the production process. A new neuronal training is necessary as soon as the nozzle type or the operating parameter has changed. Therefore, a CNN can only be applied for a nozzle and experimental setup used in the training of the CNN.

2 Material and Methods

2.1 Spray Generation

Sprays with varying droplet size distributions were generated by a hollow-cone nozzle from a commercial nasal spray applicator. The volume flow of demineralized water was adjusted by a gear pump (ISM 446, Ismatec SA, Zürich, Switzerland) leading to the desired droplet size for the creation of the image data set.

2.2 Spray Characterization

The droplet size in the spray was analyzed using laser diffraction (Spraytec STP 5921, Malvern Instruments Ltd., United Kingdom) using the Mie theory. A lens with a focal length of 300 mm was utilized, and the laser beam of the instrument arranged at a distance of 11 cm from the nozzle tip. The measurement was performed for 30 s, during which the average droplet size distribution from 30 distributions was evaluated. Each determination was conducted in triplicate.

2.3 Image Acquisition

For each flow rate (droplet size), 500 images of the spray were taken by a digital camera (Nikon Z6, Nikon Corp., Chiyoda, Japan). The spray was illuminated by two LED spotlights (KL 1600 LED, Schott AG, Mainz, Germany) placed behind the aerosol relative to the camera position (Fig. 2). Images were taken with an exposure time of 1/3200 s at a distance of 17 cm

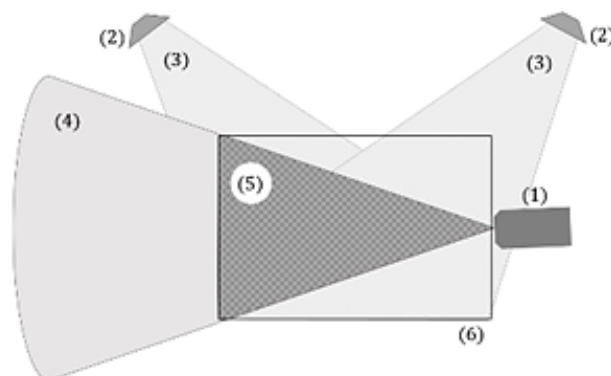


Figure 2. Experimental setup for creation of the image database. (1) Nozzle, (2) LED spotlights, (3) light cone, (4) spray cone, (5) illuminated area of the spray cone, (6) image area.

from the spray axis. A darkened room was used to prevent disturbance from ambient light. Hence, only the illuminated spray cone was visible on the resultant images, covering an area of about 15×10 cm (6048×4024 pixel). This illumination technique enabled short exposure times so that some single drops were visible on the spray images. Changes in the image acquisition like the illumination, distance, or the resolution require a new training of the CNN.

2.4 Image Evaluation

The images were converted to grayscale, and the image size was reduced by a factor of 10 to diminish computing effort. The CNN for spray categorization was trained to return the median droplet size referenced by the laser diffraction measurements. CNNs were built using the CPU version of TensorFlow version 1.13.1 (Google LLC, Mountain View, CA) and Keras version 2.2.4 on a desktop computer. The CNN designed consisted of nine layers: three convolutional and three pooling layers, two dense layers, and one output layer. The output layer consisted of five neurons, each of which represented one droplet size fraction category. Each of those neurons returned a probability based on a single image evaluation that the median droplet size was in the size category corresponding to that neuron. The category with the highest probability was defined as median droplet size determined by image analysis via CNN.

Further investigation dealt with the determination of the droplet size distribution. Therefore, the output layer of the CNN was changed by replacing the five individual output neurons with five parallel output layers consisting of five neurons each. This led to five independent probability distributions for each individual category. The probabilities represented the weight fraction of the droplets in each size class (category). A new neuronal training is necessary as soon as the nozzle type or the operating parameter has changed. Therefore, a CNN can only be applied for a nozzle and experimental setup used in the training of the CNN.

3 Results and Discussion

3.1 Determination of Median Droplet Diameter

Initial investigations dealt with the categorization of the volume-based median droplet diameter ($d_{50,3}$)¹⁾, based on spray images using CNNs. Therefore, five different sprays were generated by varying the volume flow while utilizing the same hollow-cone nozzle (Tab. 1). The flow rate was tuned such that a 20- μm difference in median droplet size was observed in the laser diffraction measurement of the previous spray. The droplet size distribution was mea-

Table 1. Parameters of spray generation: desired median droplet diameter ($d_{50,3}$ desired), volume flow rate (\dot{V}) used to adjust the spray properties, and measured median droplet diameter ($d_{50,3}$ measured).

$d_{50,3}$ desired [μm]	\dot{V} [mL min^{-1}]	$d_{50,3}$ measured [μm]
80–100	34	85.8 ± 1.2
100–120	21	105.1 ± 1.8
120–140	18	132.0 ± 6.3
140–160	17	148.0 ± 6.3
160–180	14	167.0 ± 5.1

sured via laser diffraction for each obtained spray, and the median droplet diameter ($d_{50,3}$) was determined (Tab. 1). Simultaneously, images of the spray cones were acquired using a digital camera, so data sets of 2500 images (500 repetitions of five different spray conditions) were generated. Each image was labeled with a corresponding category depending on a given $d_{50,3}$ value, as determined by laser diffraction.

Three representative raw images are given in Fig. 3, corresponding to a small (left), intermediate (center), and large (right) droplet size. The hollow-cone nozzle is positioned on the right-hand side of each image, while the spray direction is towards the left. Visual differences in the spray pattern can be recognized, and additionally, the spray angle is changing from the left to the right. These differences are used by the CNN for spray categorization.

This data set was split into an 80 % training set used to adjust the CNN to the measuring task and 20 % test set used for performance evaluation (Fig. 4). Furthermore, the training set was divided into data used for weighting the neurons (70 %) and validating the training success (30 %).

During the training of a CNN, the weights of the individual neurons are adjusted iteratively by a software algorithm until the predicted value (droplet size from CNN) and the reference value or “label” (droplet size from laser diffraction) converge. The deviation between the expected outcome and the outcome predicted by the CNN was quantified by the loss function, with y_i as the expected outcome, and \hat{y}_i representing the predicted value for class i out of n classes. y_i and \hat{y}_i are vectors of predictions containing probabilities for each class. They need to sum up to 1.

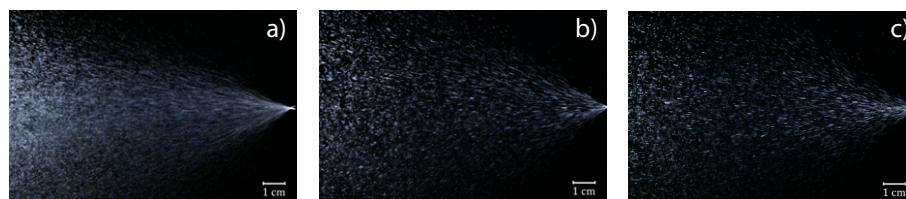


Figure 3. Representative raw images of small ($d_{50,3} = 86 \mu\text{m}$ (a)), intermediate ($d_{50,3} = 132 \mu\text{m}$ (b)), and large droplet size ($d_{50,3} = 167 \mu\text{m}$ (c)).

1) List of symbols at the end of the paper.

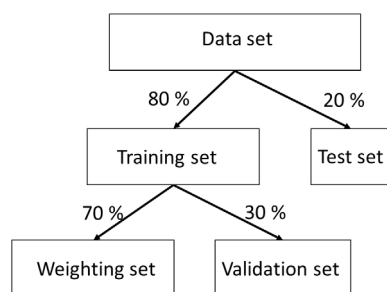


Figure 4. Division of the data set (unity of all images) into various subpopulations for weighting, validation, and evaluation (test set) purposes.

Different loss functions for various applications are commonly used and the most appropriate for image classification tasks is the so-called cross entropy (CE) loss function [17]. For the calculation of the cross-entropy, the label vectors y_i were multiplied with the logarithm of the outcome \hat{y}_i produced by the model for each of the classes and summed up. Given that n is the number of classes, the formula for the calculation of the loss for one predicted value is as follows:

$$CE(\text{loss}) = - \sum_{i=1}^n y_i \ln(\hat{y}_i) \quad (1)$$

After the weight adjustment, each training includes a validation. This gives some insight into how the CNN handles new data, but is also used to terminate training iterations. Based on this, overfitting of the CNN is avoided, leading to time-saving and higher predictive power [17]. The epochs (training iterations) of adjusting the weights and validating the success are repeated several times while training a CNN to a particular measuring task. Besides the loss value, the CNN process of learning is characterized by its accuracy. The accuracy (Eq. (2)) is determined from the validation data set, data that has not been used for weighting. The images were employed to evaluate the categorization accuracy (AC), defined as the number of the correctly predicted values N_{correct} over the total number of predictions made N_{total} .

$$AC = \frac{N_{\text{correct}}}{N_{\text{total}}} \quad (2)$$

The CNN was trained over ten epochs using randomly chosen initial weights [18] for five times under various start conditions, and similar results were obtained. The individual trainings are summarized in terms of the loss and accuracy function values of the epoch (Fig. 5). The loss characterizes the differ-

ence between the predicted value of the CNN and the value of the reference method. Low loss values indicate a good level of agreement between both categorization methods. Therefore, the loss value decreases with increasing number of epochs. The accuracy, on the other hand, is the fraction of the correctly predicted values of the CNN with respect to the reference method. Values of 1 are desired, and a value of 1 is approached by increasing the number of epochs.

Considering loss and accuracy, Fig. 5 can be used to identify the required number of training steps (epochs) to reach a given predictive power. However, too many epochs might lead to overfitting, making the CNN less flexible for interpreting new data. In this particular case of spray characterization, two to three epochs for five individual training runs with random initialization led to reasonable results (accuracy of the validation set $> 0.998 \pm 0.000$, $n = 5$) and were performed in 3 h on a desk-top computer.

Even though the loss and the accuracy indicated adequate performance of the CNN, further investigations were performed to identify the regions in the spray that contributed most to the spray categorization. This plausibility check is necessary to identify systematic artefacts, such as illumination issues. Therefore, for each image in the validation set, heat maps were created based on the algorithm of Selvaraju et al. [19]. The heat maps indicate the relevance of certain parts of the spray image for correlation with the mean droplet diameter (Fig. 6). The heat map was super-imposed on the spray image (Fig. 3) for easy interpretation.

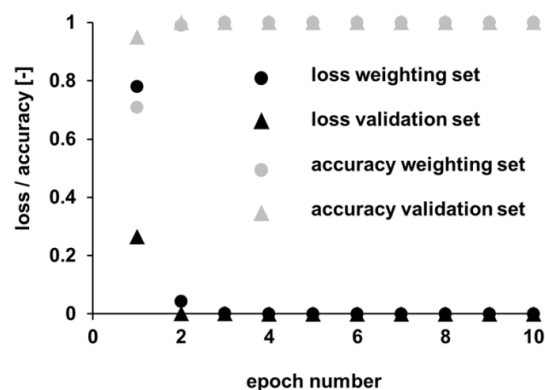


Figure 5. Performance evolution of the CNN with respect to epochs (training iterations) for categorizing the different median droplet size categories. This is a representative graph of five independent trainings.

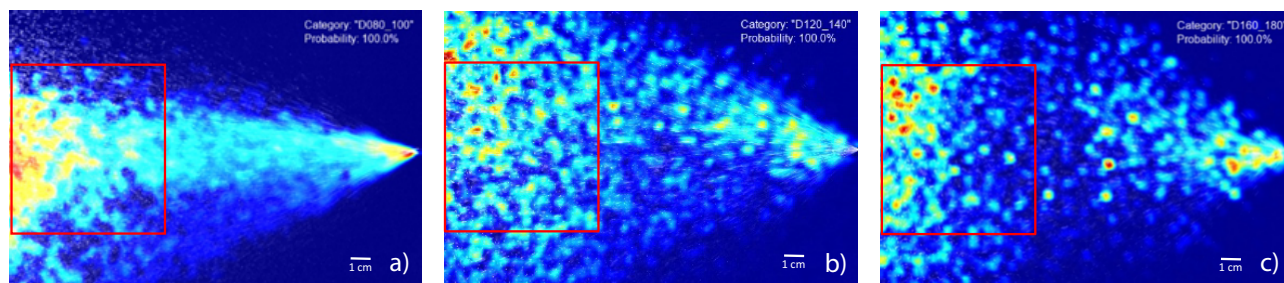


Figure 6. Representative heat map for first CNN of small ($d_{50,3} = 86 \mu\text{m}$ (a)), intermediate ($d_{50,3} = 132 \mu\text{m}$ (b)), and large droplet size ($d_{50,3} = 167 \mu\text{m}$ (c)). Red indicates relevant and blue less relevant regions in the image for CNN training.

In the heat map, some relevant areas are close to the nozzle orifice, which might be related to the deviation in the spray angle. Moreover, there is also a relevant region on the left-hand side of the image, about 100–150 mm from the orifice (Fig. 6, red box). In this region distinctive droplet clusters can be identified visually, which are reasonably believed to affect the categorization with respect to size.

Based on the evaluation of the heat maps, the region in the red square seems to be most relevant for the determination of the median droplet size. Therefore, a second CNN was trained to this subsection of the images using the original dataset.

Comparing the training results between the CNN from the entire picture (Fig. 5) and the subsections, much higher loss values (0.0392 ± 0.053 , $n = 5$) and much lower accuracies (0.987 ± 0.017 , $n = 5$) were found when using the subsections for training. These parameters also converge within six epochs, but the quality of the prediction is remarkably less. This might be related to the much lower quantity of information within the subsections. However, the second CNN may be advantageous in applications such as spray drying and spray coating processes where obtaining images in the vicinity of the nozzle is not feasible. In terms of nebulizer characterization, the use of the image subsections had limitations, because the predictive power of the CNNs based on the smaller subsets was less robust. Therefore, the first CNN was used subsequently.

The ultimate challenge for each NN is the interpretation of foreign data (test set, Fig. 4) that has not been used for training (weighting and validation). Therefore, 500 images were categorized by the first CNN and the results were compared to the image labels obtained by laser diffraction. All images were categorized correctly in accordance with the label, giving an accuracy of more than 99.8%. This test was performed five times using different trainings, and all images were categorized correctly.

3.2 Determination of Droplet Size Distribution

Since the investigations discussed in Sect. 3.1 demonstrated that sprays can be categorized to a median droplet size from images using CNNs, further investigations were conducted to determine droplet size distributions using CNNs. Therefore, the network architecture was changed from one to five output

layers, with each layer indicating an independent size fraction. For the CNN training procedure, droplet size distributions obtained by laser diffraction were utilized for image labeling. In contrast to previous investigations, the size distribution was used, rather than the median value only.

A new CNN was trained to the previous data set using the five different flow rates for the different spray characteristics given in Tab. 1. However, the categories in the output layer were adjusted to account for the width of the droplet size distribution. The bin sizes are shown on the abscissas in Fig. 7. The net was trained to five different sprays. However, only the smallest, intermediate, and largest median droplet diameters are depicted. The error bars are the standard deviations of the measurement repetitions for laser diffraction ($n = 20$) and CNN determination ($n = 100$).

The measurements of the reference method (laser diffraction) indicate a reliable spray formation and spray determination since the standard deviation of repeated measurements is low. The droplet size distribution categorized by CNN is comparable to those of the reference measurement since no relevant differences were seen between the methods. It was also observed that the droplet size produced by the nebulizer corresponded to the volume flow. A small droplet size corresponded to a high volume flow, and a large droplet size corresponded to a low volume flow. This observation is consistent with the literature [20, 21].

When comparing both techniques, laser diffraction can be seen as the gold standard in droplet size evaluation. However, the measuring equipment is delicate, expensive, and usually meant for a lab environment rather than for harsh production conditions. Appropriate sample preparation is the key for a meaningful measurement. Image analysis using CNN is a new technique that is rapidly emerging in many applications in our daily life, ranging from traffic signs to face detection. The equipment is cheap, i.e., single-board computers such as the Raspberry Pi and Jetson nano can be obtained for less than €100 including the digital camera. However, there is more effort required to establish a new measuring task for these systems, because the CNNs must be created. Slight changes in data acquisition can alter the quality of the results. Therefore, constant validation is needed, but no sample preparation is required. Additionally, the cameras can be implemented into many manufacturing processes such as spray drying and spray

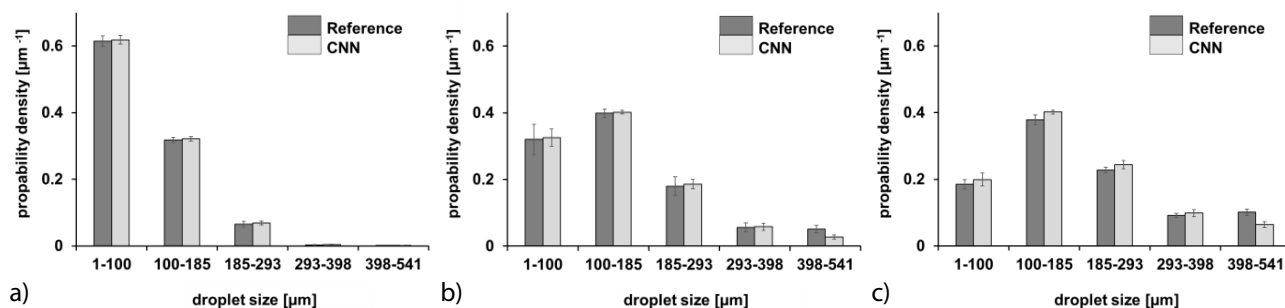


Figure 7. Representative droplet size distributions obtained by laser diffraction measurements (reference, $av \pm s$, $n = 20$) and CNN determination ($av \pm s$, $n = 100$) corresponding to small ($d_{50,3} = 86 \mu\text{m}$ (a)), intermediate ($d_{50,3} = 132 \mu\text{m}$ (b)), and large ($d_{50,3} = 167 \mu\text{m}$ (c)) median droplet size.

coating. Real time data can also be acquired, enabling feed forward and feed backward control strategies based on high sampling rates.

Overall, image analysis by CNN is a versatile and powerful technique and comparable to laser diffraction with respect to the results. However, it is more suited for an in-line production environment for process or product control applications, rather than as lab equipment for droplet size categorization of different samples.

4 Conclusion

A method of spray categorization from images using CNNs was introduced. Open-source software and a desktop computer were utilized. Laser light diffraction served as the reference method while different sprays were formed using various flow rates and a commercial hollow-cone nozzle.

Initial experiments dealt with the determination of the median droplet size. Therefore, an automated iterative training was performed using 2000 spray images and corresponding laser diffraction data, which took several hours. The trained CNN was then applied to categorize the median droplet size in 500 images that had not been used for training, and all images were predicted correctly.

Further investigation dealt with the determination of the droplet size distribution, which required a new CNN architecture as well as an additional screening. The droplet size distributions of 100 images were also categorized correctly, while no relevant differences to the reference measurement were found.

Image analysis using CNNs is a promising approach for spray characterization, as it requires no sample preparation, is fast, and has in-line capabilities.

Data Availability Statement

The data that support the findings of this study are available from the corresponding author upon reasonable request.

Acknowledgment

Open access funding enabled and organized by Projekt DEAL.

The authors have declared no conflict of interest.

Symbols used

$d_{50,3}$	[μm]	volume-based median diameter
y	[-]	labeled value
\hat{y}	[-]	predicted value by the CNN

Abbreviations

CNN	convolutional neural network
NN	neural network

References

- [1] *Atomization and sprays* (Eds: A. H. Lefebvre, V. G. McDonnell), CRC Press, Boca Raton, FL **2017**.
- [2] Y. S. Cheng, T. D. Holmes, J. Gao, R. A. Guilmette, *J. Aerosol Med.* **2001**, *14* (2), 267–280.
- [3] P. J. Anderson, J. D. Wilson, F. C. Hiller, *Chest* **1990**, *97*, 1115–1120. DOI: <https://doi.org/10.1378/chest.97.5.1115>
- [4] P. Zanen, L. T. Go, J. W. Lammers, *Thorax* **1996**, *51*, 977–980.
- [5] S. Trows, K. Wuchner, R. Spycher, H. Steckel, *Pharmaceutics* **2014**, *6*, 195–219. DOI: <https://doi.org/10.3390/pharmaceutics.6020195>
- [6] S. Deshpande, A. Kulkarni, S. Sampath, H. Herman, *Surf. Coat. Technol.* **2004**, *187*, 6–16.
- [7] A. Kavian, M. Mohammadi, A. Cerda, M. Fallah, Z. Abdollahi, *CATENA* **2018**, *167*, 190–197.
- [8] J. B. Blaisot, J. Yon, *Exp. Fluids* **2005**, *39*, 977–994.
- [9] S. Maaß, J. Rojahn, R. Hänsch, M. Kraume, *Comput. Chem. Eng.* **2012**, *45*, 27–37.
- [10] I. H. Sarker, *SN Comput. Sci.* **2021**, *160*, 1–21.
- [11] S. Unnikrishnan, J. Donovan, R. Macpherson, D. Tormey, *IEEE Trans. Ind. Inf.* **2020**, *1*, 1–6. DOI: <https://doi.org/10.1109/TII.2019.2959021>
- [12] *Deep Learning. Das umfassende Handbuch: Grundlagen, aktuelle Verfahren und Algorithmen, neue Forschungsansätze*, 1st ed. (Eds: I. Goodfellow, Y. Bengio, A. Courville), mitp, Frechen, Germany **2018**.
- [13] V. Dumoulin, F. Visin, *A guide to convolution arithmetic for deep learning*, ArXiv, **2016**. Corpus ID: 6662846
- [14] M. Al-Qizwini, I. Barjasteh, H. Al-Qassab, H. Radha, *IEEE Intell. Vehicles Symp.* **2017**, *4*, 89–96.
- [15] A. Esteva, B. Kuprel, R. A. Novoa, J. Ko, S. M. Swetter, H. M. Blau, S. Thrun, *Nature* **2017**, *542*, 115–118.
- [16] K.-Su Oh, K. Jung, *GPU implementation of neural networks*, *Pattern Recognition* **2004**, *37* (6), 1311–1314.
- [17] *Deep Learning mit Python und Keras*, 1st ed. (Eds: F. Chollet, K. Lorenzen), EBSCO Industries, Frechen **2018**.
- [18] A. Saxe, P. W. Koh, Z. Chen, M. Bhand, B. Suresh, A. Ng, *ICML* **2011**, 1089–1096.
- [19] R. R. Selvaraju, M. Cogswell, A. Das, R. Vedantam, D. Parikh, D. Batra, *Int. J. Comput. Vision* **2020**, *128*, 336–359.
- [20] P. Walzel, *VDI-Wärmeatlas*, Springer, Berlin **2019**, 1661–1682.
- [21] W. C. Hinds, *Aerosol Technology. Properties, Behavior, and Measurement of Airborne Particles*, 2nd ed., Wiley-Interscience, **1999**.